Chapter 6

Synthesis of Fe_3O_4 Nanoparticles using *edta* as Template, Their Characterization and Applications as Vectors for Gene Delivery

6.1 Introduction

Transfection of foreign plasmid or RNA into host cell nucleus is very much important nowadays, for the production of required protein in situ, in the cells only. This cost affecting technique is also important for the large scale production of protein industrially and also in the treatment of diseases like cystic fibrosis,[1] immune deficiency, hemophilia A causing due to gene mutation.[2] However, this is not an easy task, eg. Nucleases like cellular enzymes immediately degrade such plasmids on the way before targeting to the nucleus (Figure 6.1) [3; 4; 5; 6]

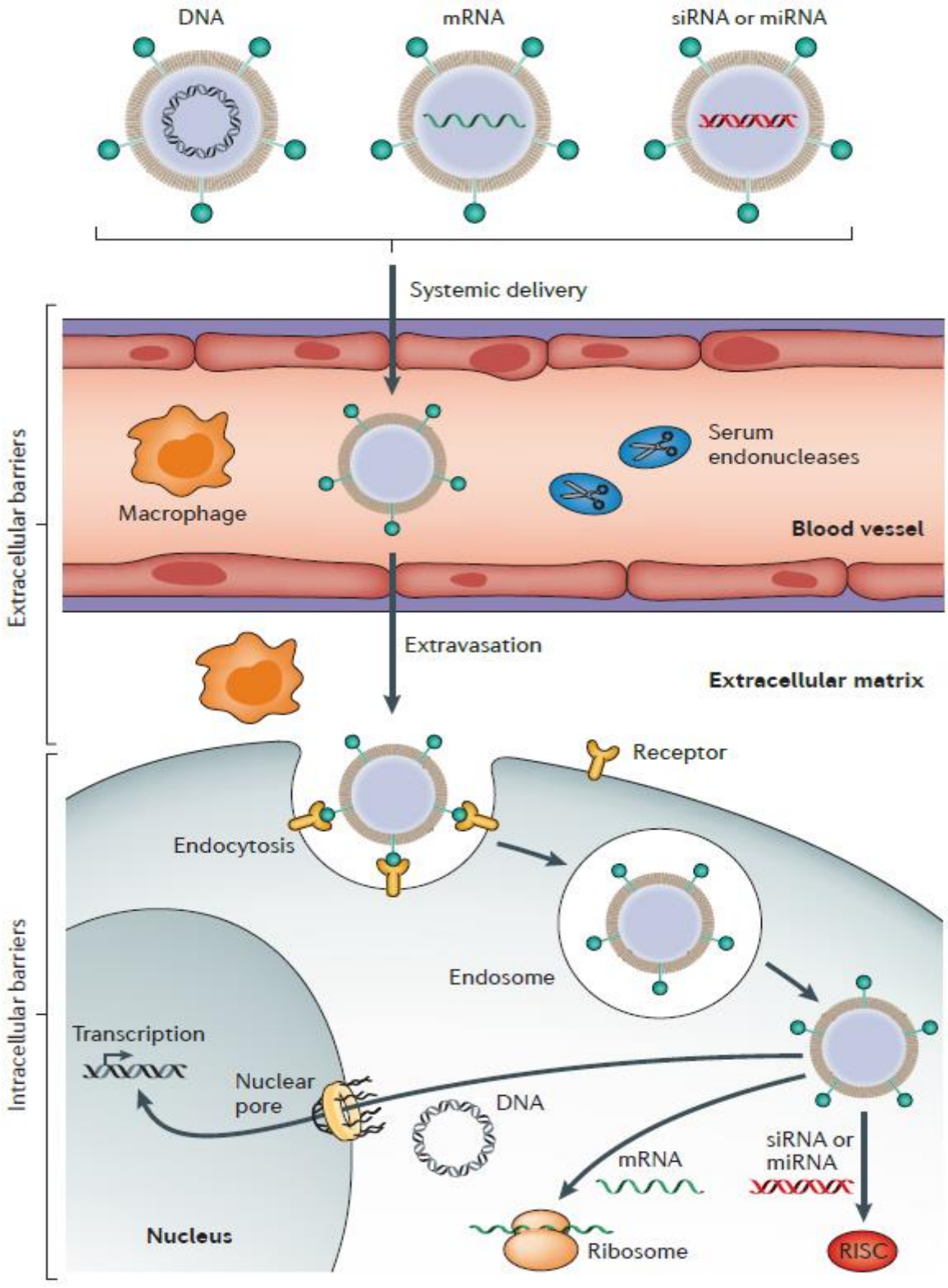

Figure 6.1.**Barriers to successful *in vivo* delivery of nucleic acids using non-viral vectors.***Various non-viral vectors can be used to deliver DNA, mRNA and short double-stranded*

RNA, including small interfering RNA (siRNA) and microRNA (miRNA) mimics. These vectors need to prevent degradation by serum endonucleases and evade immune detection (which could be achieved by chemical modifications of nucleic acids and encapsulation of vectors). They also need to avoid renal clearance from the blood and prevent nonspecific interactions (using polyethylene glycol (PEG) or through specific characteristics of particles). Moreover, these vectors need to extravasate from the bloodstream to reach target tissues (which requires certain characteristics of particles and specific ligands), and mediate cell entry and endosomal escape (by specific ligands and key components of carriers). siRNA and miRNA mimics must be loaded into the RNA-induced silencing complex (RISC), whereas mRNA must bind to the translational machinery. DNA has to be further transported to the nucleus to exert its activity (Hao Yin, R L Kanasty, A AEltoukhy, A J Vegas, J R Dorkin, D G Anderson, Non-viral vectors for gene-based therapy, Nature Reviews Genetics | AOP, published online 15 July 2014; doi:10.1038/nrg3763).

The only viable solution of this problem is to insert the required plasmid or RNA in the vehicle (either synthesized or from natural origin) which can easily extravasate the cell membrane and sustainable enough to reach to the nucleus before degradation by nucleases. Viruses are the naturally evolved machinery ideal for this purpose.[7; 8] Viral vectors like retroviruses, lentiviruses, adenoviruses and adino-associated viruses were developed consequently.[9; 10]However, the drawback with these carriers is that the human body may develop immunity against such viruses, degrade the same and barriers due to carcinogenesis and recombination efficiency are also limit the wide use of these viral vectors.[11; 12] These result into the requirement of safe and non-toxic non-viral gene delivery vectors non-viral

vectors have low transfection capacity, however, as they cannot sustain against multiple barriers (eg macrophage, serum endo-nucleases, filtration and exist through glomerular system etc) during transfection. Lot of efforts has been carried out in the direction towards the development of safer and efficient non-viral vectors. From all of developed non-viral vectors lipid based (liposomes) and polymer based (polymersomes) are major. For example cationic lipids like DOTAP(N-[1-(2,3-Dioleoyloxy)propyl]-N,N,N-trimethylammonium methyl-sulfate), DMRIE ((1,2-dimyristyloxy-propyl-3-dimethyl-hydroxy ethyl ammonium bromide), DOTMA (N-[1-(2, 3-dioleyloxy)propyl]-N,N,N-trimethylammonium chloride), DC-cholesterol etc having hydrophilic cationic head group, hydrophobic long hydrocarbon chains and linker group between the two have a capability to entrap DNA within the self-assembled lamellar bilayers (Figure 6.2).

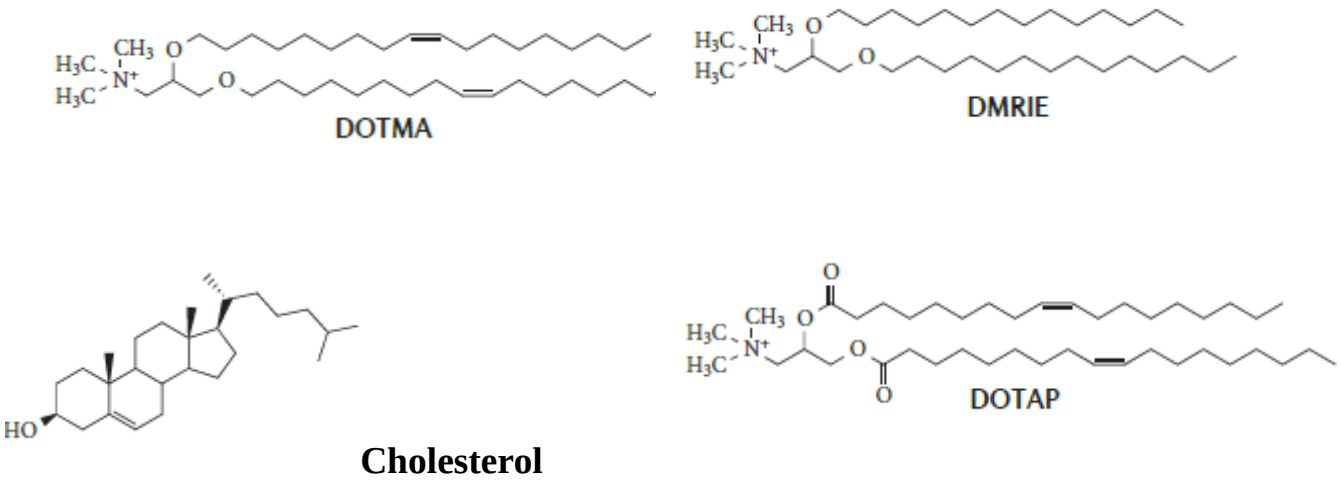

Figure 6.2. Chemical structure of some cationic lipids used for gene transfection purpose.

However, low delivery efficiency, poor stability and rapid renal clearance are the drawbacks associated with these liposomal delivery vectors.[13; 14] Synthetic or natural polymers having a capacity of forming self-assembly are also emerged as gene delivery vectors. For example, poly(L-lysine) (PLL) and its block copolymer with polyethylene glycol (PLL-b-PEG),[15; 16; 17] poly ethyleneimine (PEI),[18][19; 20; 21] PAGA (poly[α-(4-aminobutyl)-l-glycolic acid,[22] PAMAM (polyamidoamine) type dendrimers[23; 24]etc have shown their capability to fuse covalently or electrostatically with DNA and acting as non-viral gene delivery vectors. Polymers from carbohydrate class such as chitosan, poly-β-cyclodextrin[25; 26; 27; 28] were also demonstrated for the purpose. However, issues corresponding to efficiency and safety still remain as challenge inviting further research in the field.

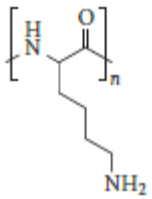

Poly(L-lysine)

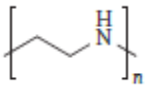

Linear PEI

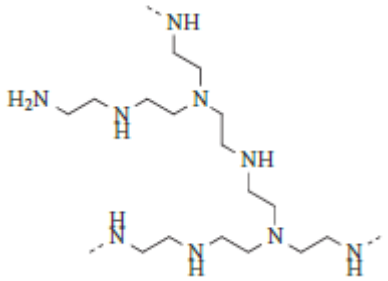

PEI with branch chains

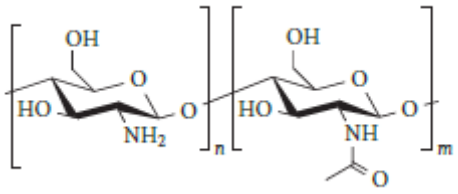

Chitosan

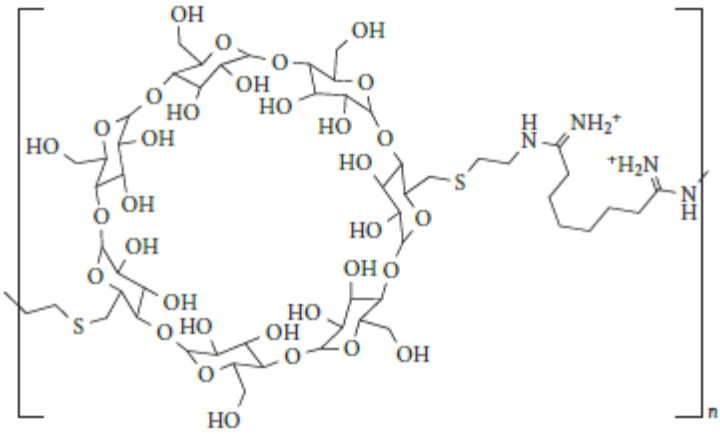

B-cyclodextrin-cage

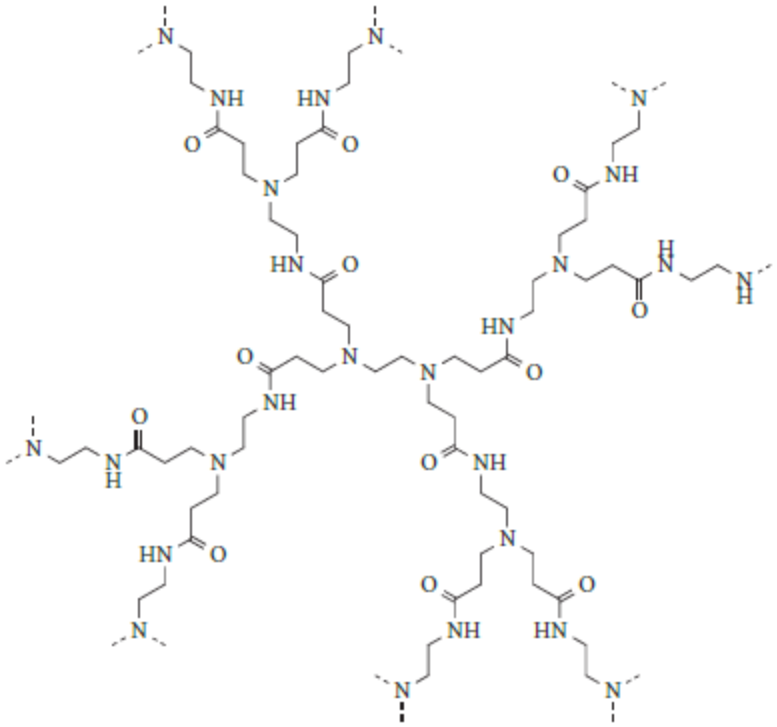

PAMAM dendrimer

Physical methods are also applied to make the cells competent forgene transformation. For example,the cells can be made competent thorough electroporationand/or mild heat shock.[29] Plasmids are also introduced into *E.Coli* through hydrogel exposure method.[30]The cell transformation can also be carried out through narrow polymer membrane pores under external electric field or hydrodynamic pressure.[31] Actually, the mechanism by which DNA is taken up by bacterial cells is still uncertain and many theories have been proposed. Hanahan *et al*. proposed that bacteria (E. coli) can take up DNA in double-stranded form.[32] It

is also to be noted that divalent cations are thought to play an important and sometimes essential role in the early stages of DNA uptake; hence the use of calcium ions is mentioned protocol.[33]Some theory suggests that DNA requires channel to enter into the bacterial cells. While some propose that plasmid DNA may not require any form of channel. Instead of simply being allowed to approach a bacterial membrane, the plasmid can allow loops of DNA to pass through the lipid bilayer into the cytoplasm of the cell.This initial action is followed by subsequent loops entering the cell until the entire length of the plasmid has passed through the membrane. Lastly, it has been suggested that an open-circular form of plasmid DNA may be able to use the calcium channels to enter a bacterial cell. In knowing that, the trivalent cations spermine and sperimidine, when used at specific concentrations, were capable of condensing plasmid DNA into spherical clusters.[33]

Transformation applying magnetic field to obtain rapid contact between the vectors and target cells have been described by Luo and Saltzman in 2000.[34]Bulk iron oxide are found to exhibit muti-domain ferromagnetism (exhibits permanent magnetism even in absence of magnetic field) whereas iron oxide NPs having size 20-30nm have single magnetic moment and exhibit superparamagnetism.[35]

In our study *E.Coli* transformation was carried out using superparamagnetic Fe_3O_4 nanoparticles under the influence of magnet. The advantage with regard to magnetofection is that a competent cell preparation is not required. The purpose of this study is to develop a transformation technique wherein potential iron oxide nanoparticles acts as carrier to pDNA and transforms it into bacterial host cells. However, this study may need to be further extended to eukaryotic cells also. Three different plasmids pBSKS, pTX and pUC18, [36]containing ampicillin resistance genes, were isolated from *E. coli* culture. These plasmids were eluted, purified, and utilized for loading on the surface of Fe_3O_4 nanoparticles. Such gene loaded Fe_3O_4 nanoparticles were transformed into *E. coli DH5α.* As an evidence of successful transformation, bacteria under study demonstrated the excepted resistance against the antibiotics.[37; 38] Enhanced green fluorescence protein tag was attached with pUC18 as marker and confocal microscopy of the pUC18*egfp* transformed *E. coli DH5α* strain was carried out to confirm the successful transfection. In this work, we have presented direct evidence of cell transformation by using plasmid-loaded Fe_3O_4 nanoparticles.

6.2 Experimental

6.2.1 Materials

Ferric Chloride ($FeCl_3.6H_2O$) was obtained from Loba chemicals, India. Ferrous Chloride ($FeCl_2.2H_2O$),Ethylene diamminetetraacetate (*edta*) and sodium

hydroxide (NaOH) were purchased from S D Fine Chemicals, India. Pluronic F-127 was purchased from Sigma Aldrich. All chemicals were AR grade and used without further purification. Chloroform, phenol, isopropanol was purchased from Merck.

6.2.2 Synthesis of Fe_3O_4/*edta*NPs

Fe_3O_4 NPs were synthesized by simple co-precipitation method. Aqueous solution of hydrochloric acid (400µL of 0.32M HCl) was dropwise added to the mixture of 50 mL aqueous solution of $FeCl_3$.$6H_2O$ (0.24 mmol) and $FeCl_2.2H_2O$ (0.121 mmol). To this solution, 25 mL of aqueous solution of EDTA (0.24 mmol) was added and the temperature of reaction mixture was gradually raised to 70 ^oC. The reaction mixture was further stirred thoroughly for about 1 h to obtain a homogenous mixture. To this solution, 25 mL 1M NaOH solution was added dropwise. The reaction mixture was further stirred for 24 h to obtain stable homogenized dispersion. The reaction mixture was then centrifuged at 8000 rpm for 5 min and subsequently washed several times with water and ethanol to remove unreacted impurities and dried at 70 ^oC under vacuum for two days.

6.3 Characterization of synthesized Fe_3O_4/*edta*NPs.

X-ray powder diffraction (XRD) pattern of the Fe_3O_4/*edta* NPs were obtained from X-ray powder diffractometer (Bruker D8 Advance) with Cu Kα radiation, λ = 0.15418 nm. The compositional analysis of the powder samples was carried out

using EnergyDispersive X-ray analyses (EDX, Jeol 8086).The mode of interaction of *edta* with the surface Fe ions of Fe_3O_4 NPs and the structure of magnetic micelles were assessed by Fourier transform infrared spectroscopy (RX-FTIR, Perkin- Elmer, USA). The morphology of the samples was examined by transmission electron microscopy (TEM, Philips Tecnai 20) at 200 kV. The hydrodynamic size, size distribution and surface charge in term of zeta potential (ζ) were measured using a dynamic light scattering (DLS) technique at a scattering angle of 90^o. A BIC 90 plus (Brookhaven) equipped with 35.0 mW solid state laser operating at 660 nm and an avalanche photodiode detector was used for the purpose. All measurements were made at 25 ^oC in deionized water. Differential Scanning Calorimetric (DSC) analysis and ThermoGravimetric Analysis (TGA) of Fe_3O_4/edta and Fe_3O_4/edta/P samples were carried out using Mettler Toledo DSC 822. For the purpose, the material was heated inside a DSC setup. The heating rate was 10 $^oC\ min^{-1}$ from RT to 500 ^oC in N_2 atmosphere. The magnetic properties were studied on a vibrating sample magnetometer (VSM, Lakeshore 7410) at 298 K under an applied magnetic field of 15.000E+3 G.

6.3.1 Isolation, detection and purification pDNA

6.3.1.1 Harvesting the bacterial culture

In order to obtain cell culture for isolation of plasmid DNA, the cells were to be harvested. First a pure culture was obtained by streaking *Ecoli* culture on lb agar plate having ampicillin by four flame method, to ensure that single well isolated were obtained. One-three such isolated colony was taken in the wire loop and inoculated in 100 ml autoclaved lb broth containing required antibiotic(5µg/ml) which was added under laminar air flow unit. It was then kept for incubation at 37^{o}C overnight to allow uniform aeration and growth of bacterial culture.

6.3.1.2 Isolation, detection of plasmid:

Plasmid isolation from *E. Coli*

Alkalysis method for isolation of plasmid from *E.Coli* has been followed (Sambrook and Russell, 2001):

The bacterial cells were harvested to obtain the culture for isolation of plasmid DNA.2 ml over night grown *E.coli DH5α* culture was pelleted down. 100 µl of AL-1 was added to the pellet and vortexed vigorously. 200 µl AL-II was added and mixed well. 150 µl AL-III was added and mixed well, stored on ice for 10 min. Centrifuged at 9K/5’ and collected supernatant. It was extracted with one volume of Phenol: Chloroform (1:1). Centrifuged at 9K/5’ and the upper aqueous layer was

transferred in fresh eppendorf. It was then extracted with one volume of Chloroform. Centrifuge at 9K/5' and again collect the upper aqueous layer. One volume of Isopropanol was added to it and incubated at -20 °C for 30'. Centrifuge at 9K/5' and supernatant was discarded. Washed once with 75% ethanol and evaporated the ethanol completely. Finally pellet was resuspended in autoclaved DDW (~20 µl).

6.3.1.3 Detection of plasmid DNA on Agarose Gel Electrophoresis :

The plasmid DNA samples isolated were loaded along with buffer and bromophenol blue dye on 1.0% agarose gel and observed on UV trans illuminator for qualitative analysis of plasmid isolated.

6.3.1.4 Transformation of plasmid DNA in *E.coli* (Sambrook and Russell, 2001)

Inoculated 3 ml LB with *E.coli DH5α* and incubated at 37ºC till it reaches OD ~ 0.4 - 0.6 (log phase). 3 ml log phase culture of *E.coli* was pelleted down at 5000 rpm/5min. Transformation was also carried out through magnetofection method. In this method the *E. Coli* in log phase was pelleted down at 5000 rpm/5min and then washed. Added DNA functionalized NPs and heat shock was given at 42^{o}C for 90 seconds and immediately transferred on ice for 2-3 minutes and then 800 µl of sterile luria broth (LB) was added and incubated at 37^{o}C for 45 minutes under

shaking conditions with magnet below the flask. Pellet down the cells and resuspend in 40µl LB. Spread it on luria agar plates containing ampicillin.

6.4 Formulation of nanoparticle

Fe_3O_4 nanoparticles were prepared using chemical wet method. To these nanoparticles (2 mg/ml) 999 µl of 20% PEG-NaCl binding buffer and 1µl of DNA (700ng/µl) were added to it. And then it was further incubated at room temperature for about 5 minutes.

Then after the contents were vortex for 1 minute to remove unbounded DNA. The supernatant obtained was transferred in another eppendorf to estimate the amount of $Fe_3O_4$and DNA that failed to assemble into nanoparticles.

6.5 Transformation of pDNA loaded Fe_3O_4 nanoparticles into *E.coliDH5α.*

6.5.1 Coinoculation of DNA loaded nanoparticles with DH5α

For the uptake of nanoparticles by bacteria, 50 µl of overnight grown pure culture was inoculated in agar-agar plate(2 g/100ml) containing 200 µl of nanoparticles solution that was added through filter, under LAFU. This culture was allowed to grow over night, at 37^{o}C with constant shaking under the influence of magnet.

6.5.2 Screening of transformants.

To screen the transformants for uptake of plasmid loaded onto the nanoparticles, about 50µL of culture was aspirated and added to the plate containing ampicillin.

This was allowed to grow over night on shaker incubator at 37^{o}C. The growth of bacteria confirmed the uptake of plasmid with ampicillin resistance plasmid loaded onto the nanoparticles. The samples were also analyzed by TEM images.

6.6. Results and Discussion

The synthesized iron oxide nanoparticles were characterized by XRD to study crystallinity and phase of the material (Fig. 6.3). The XRD patterns manifest predominant diffraction peaks at 2θ values30.1, 35.15, 43.10, 53.50, 57.21 and 63.0 correspond to the (200), (311), (400), (422), (511), and (440) planes, respectively. These features indicate the magnetite phase with inverse spinel structure in which oxygen forming cubic face centered packed (FCC) arrangement and Fe cations occupy the interstitial Td and Oh sites. These standard peak positions indicate that coating of *edta* on Fe_3O_4 NPs as capping ligands does not affect the phase and crystallinity of the material. The particle size calculated from Debye-Scherrer formula ($L=0.9\lambda / \beta \cos\theta$) and the FWHM (Full Width at Half Maximum) values corresponds to the major plane (311) was in the range of 56 nm. The compactness and clear resolution of the peaks indicate properly ordered and compact *edta* layer on the surface of NPs.

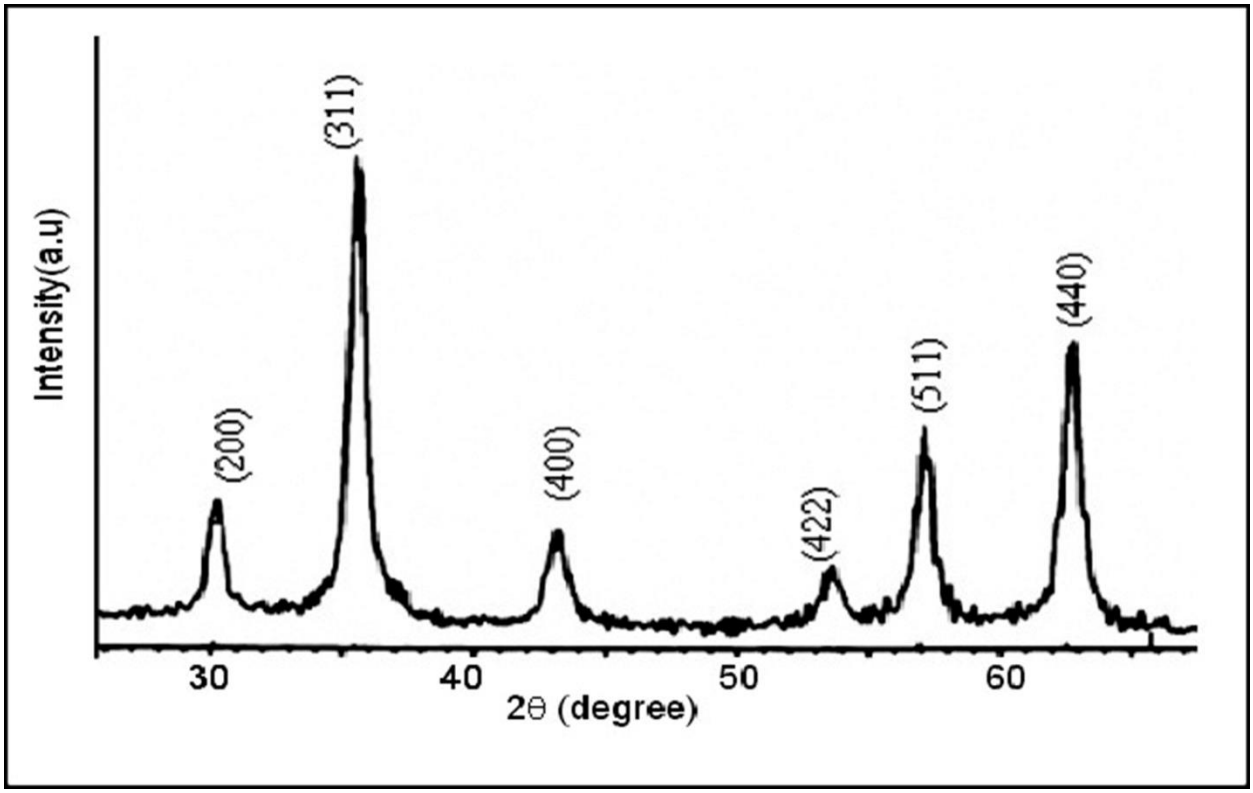

Fig.6.3 XRD patterns of as-synthesized Fe_3O_4/*edta* nanoparticles.

Further, the size and shape of Fe_3O_4/*edta* NPs were studied by TEM analysis. The TEM image shows almost monodispersed spherical particles with an average size 5-10 nm (Fig. 6.4). Particle size was further measured by dynamic laser light scattering technique (Fig. 6.S1). The mean particle size for Fe_3O_4/*edta* NPs was 232 nm with polydispersity index 0.251. On addition of pluronic the average particle size increases to 440 nm with polydispersity index 0.005. The discrepancy in particle size measure by DLS and that of XRD and TEM was very well explained by Jain at al. DLS measures overall hydrodynamic diameter of the NPs assembly resulted from hydration of Fe_3O_4/*edta* with aqueous media in first case

while Fe_3O_4/*edta*/P with aqueous media for second case. The small value of polydispersity index for Fe_3O_4/*edta*/P system suggests ordered orientation of NPs assembly in aqueous media. In this study, *edta* plays dual role, first it acts as a capping agent and restrict the growth of Fe_3O_4 crystal to the nano regime. Secondly, *edta* can increase the dissociation rate of Fe_3O_4 NPs, mineralize it completely and merge the same into the blood pool, by this way it can reduce the toxicity of the material.

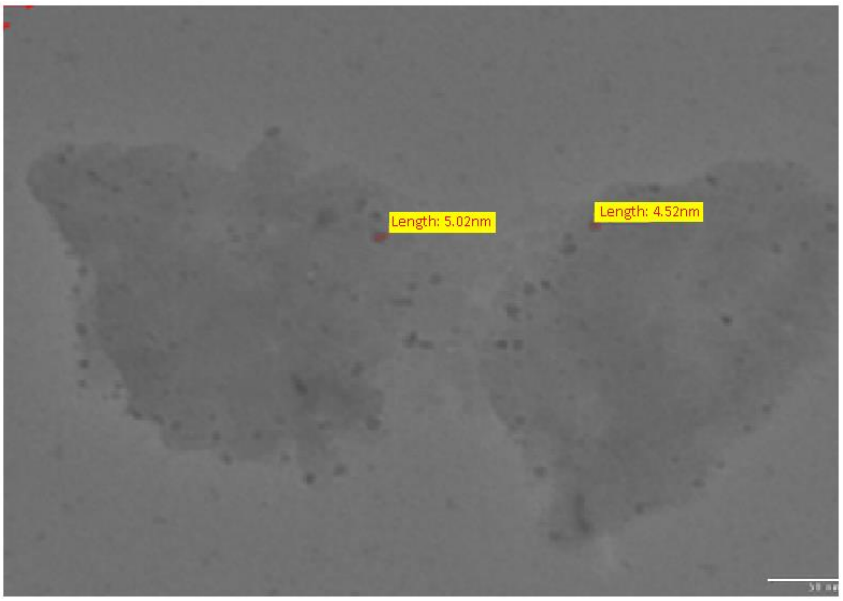

Fig.6.4 TEM image of as-synthesized Fe_3O_4/*edta* nanoparticles.

To understand the interactions of the *edta* ligands with the surface of Fe_3O_4 NPs, vibrational spectroscopy (FTIR) is one of the best tools. Figure 6.S2 shows the FTIR spectrum of Fe_3O_4/*edta* , Fe_3O_4/*edta*/pTX and Fe_3O_4/*edta*/pBSKS assembly respectively. The absorption at 646 cm^{-1} (Fig 6.S2) is corresponds to Fe-O

stretching in Fe_3O_4 inverse spinel system. *edta* possesses two nitrogen atoms and four carboxylate anions (in basic media) to coordinate with surface iron (II/III) ions. The four carboxylate ions can coordinate with surface iron ions either in a unidentate or a bidentate (chelating) ways. This can be confirmed on the basis of COO^- stretching vibration frequencies. Carboxylate ions in free acetate form vibrate in two fundamental modes, asymmetric stretching $\nu_{as\,(COO^-)}$ and symmetric stretching $\nu_{s\,(COO^-)}$ at 1583 and 1422 cm^{-1} respectively. If carboxylate ligand coordinate with surface Fe (II/III) as a bidentate mode then $\nu_{as\,(COO^-)}$ decreases and $\nu_{s\,(COO^-)}$ increases from the above normal modes in free state and vice versa in case of monodentate mode. On comparing Δ ($\nu_{as\,(COO^-)}$ - $\nu_{s\,(COO^-)}$) with Δ'($\nu'_{as\,(COO^-)}$– $\nu'_{s\,(COO^-)}$), (where Δ is a difference in the absorption bands for free carboxylate ions and Δ' is for metal bound carboxylate ions), we found $\Delta>\Delta'$. This suggests bidentate coordination.

It can be observed that pristine Fe_3O_4/*edta* NPs possesses negatively charged surface with ζ value -23.87 mV and when bounded with pBSKS and pUC18 it decreases to -14.73 mV and -9.27mV respectively. It was observed that the emergence of charge on the surface is directly influenced by the presence of counter ions in the medium and the mode of crystallization. Obviously, the negative charge on the surface of pristine Fe_3O_4/*edta* is due to presence of ^-OH ions in the basic aqueous medium. During the crystal growth, ^-OH ions as well as

edta both act as capping ligands, however, ¯OH ions are more prone to be adsorbed on the surface while *edta* makes coordination with surface Fe (II/III) ions.

Magnetic properties of the synthesized Fe_3O_4/*edta*. The shape of magnetization curve (Fig. 6.5) indicates superparamagnetic behavior in presence of magnetic field. The magnetization and coercivity of Fe_3O_4/*edta* NPs were 0.4 emu/gm and 0.4611 G (Hci).

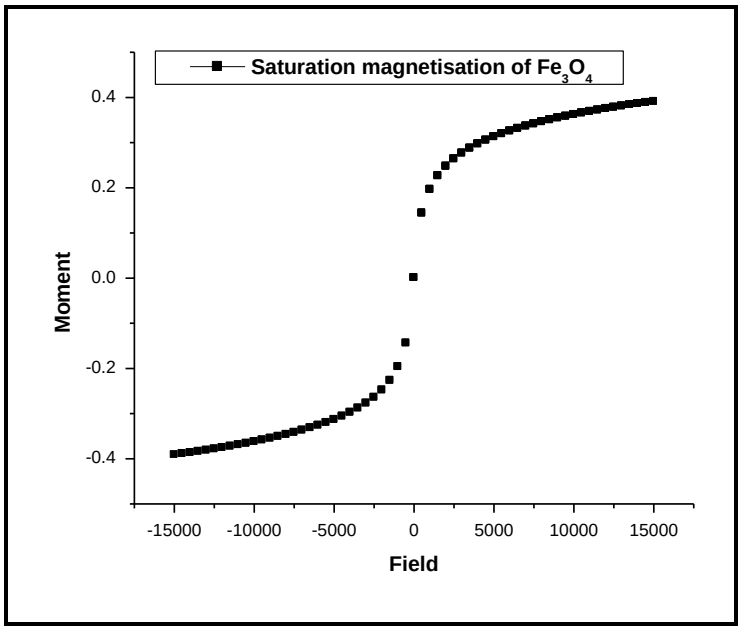

Figure 6.5 :Magnetization curve at room temperature for EDTA/Fe_3O_4 nanoparticles.

Evaluation of pDNA.

The concentration and purity of plasmid DNA was measured by using UV-Visible spectrophotometric method. In this method, 50µL of plasmid DNA solution was mixed gently with 2950 µL of distilled water and the absorption of these samples was measured at 260 nm and 280nm.

$$\text{Concentration of DNA (ng/µL)} = \frac{\text{Absorption at 260 nm X dilution factor X 50}}{1000} \quad (1)$$

The ratio of the 260: 280 nm absorption found around 1.9 implies that the DNA was pure, and

no RNA or protein impurity was present in the sample. Concentration of DNA was measured at 260 nm absorption. Agarose electrophoresis was carried out in order to confirm thesize of the eluted plasmid DNA.

Evaluation of plasmid DNA loaded nanoparticles

The amount of plasmid DNA loaded into Fe_3O_4 particles was calculated as the difference between the total amount of the initial plasmid DNA added and the amount of plasmid DNA present in the supernatants obtained during the purification step by spectrophotometer at 260 nm.

Concentration of DNA loaded was calculated. pBSKS loaded on the surface of nanoparticles is 394 ng/mg, pTX loaded on the surface is 426ng/mg and pUC18 loaded on the surface of nanoparticles is 412ng/mg.

Total 50 µl of pDNA was added in the formulation. pDNA loaded Fe_3O_4 NPs were suspended in 300 µl of phosphate buffer saline (PBS) of pH 7.4 as release media in an eppendrof and was placed in shaking water bath at 37^{o}C with a constant rotation of 60 rpm. At predetermined intervals, 50 µl samples were withdrawn and replaced with 50 µl fresh media in the eppendrof. The amount of DNA released was determined by centrifuging it and supernatant obtained was analyzed by using spectrophotometer at 260 nm.

$$\%Release\ of\ pDNA = \frac{Amount\ of\ pDNA\ released}{Amount\ of\ pDNA\ present\ in\ NPs} \quad \ldots\ldots\ldots \quad (2)$$

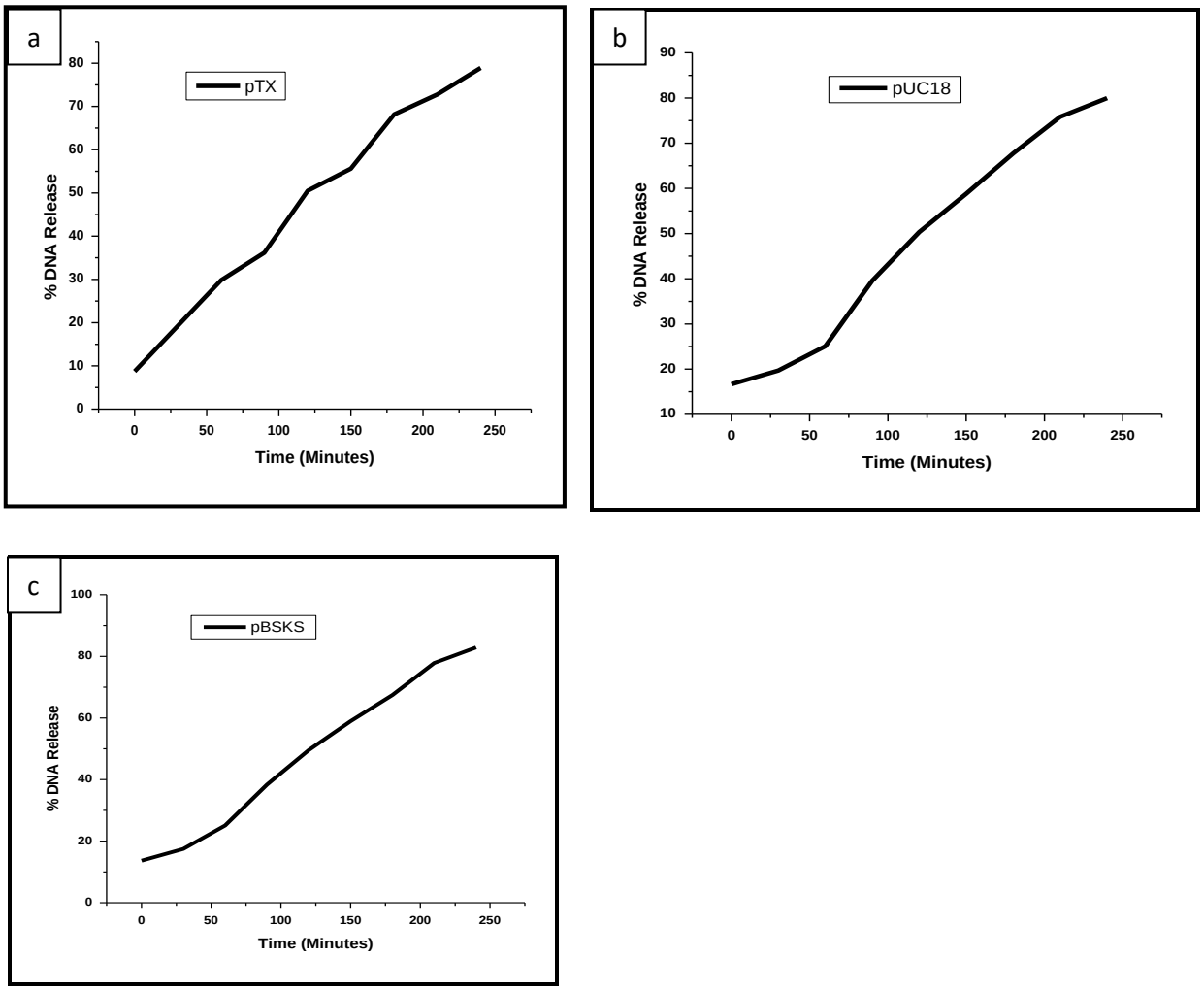

Figure 6.6 Release profile of (a) pTX , (b) pUC18 and (c)pBSKS loaded Fe_3O_4 nanoparticles

From the zeta potential values, the mechanism of interaction of Fe_3O_4-NPs with pDNA can be expected.

Table 1. Zeta potential of Fe_3O_4 nanoparticles loaded with different plasmids.

Nanoparticles	Loaded with plasmid	Zeta potential (mV)
Fe_3O_4	-	-52.21
	pUC18	-40.2
	pTX	-19.27.
	pBSKS	-33.56

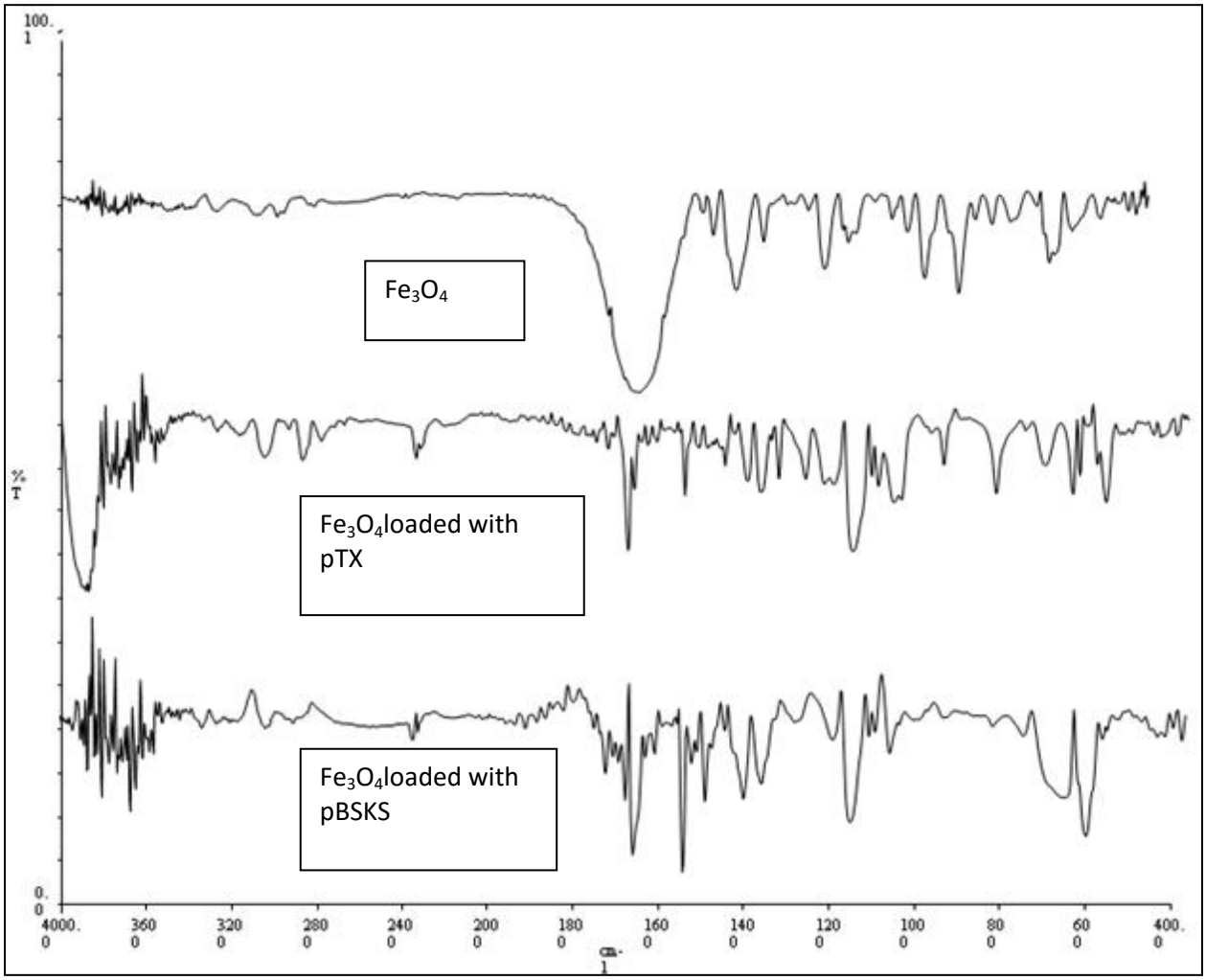

Figure :6.S2 FTIR spectra of Fe_3O_4/*edta* NPs, Fe_3O_4 loaded with pTX NPs and Fe_3O_4 loaded with pBSKS NPs

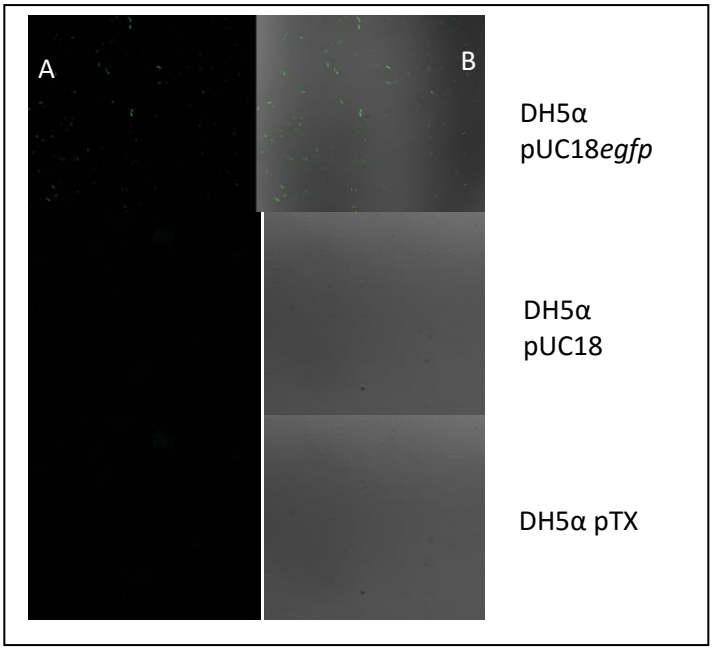

Figure 6.7: Confocal microscope images of DH5α transformed with pDNA. A-lane fluorescent filed and B-lane merges of fluorescence and bright field.

It is logical to think that if the transformation is successfully done then the bacteria should adapt the resistance towards antibiotics. For the purpose, the transformed *E. coli* DH5α strain was grown in ampicillin containing plate. It can be seen from the figure below that the pDNA transformed colonies were grown on ampicillin or kanamycin antibiotic containing plates to which they were susceptible previously. Further, the transferred plasmid was again isolated from these *E.coli* strain to prove

the integrity of the plasmid during the transfection process and the results show retention of function of pDNA (in figure below). This proves Fe_3O_4 NPs as a promising candidate for successful gene delivery for cells.

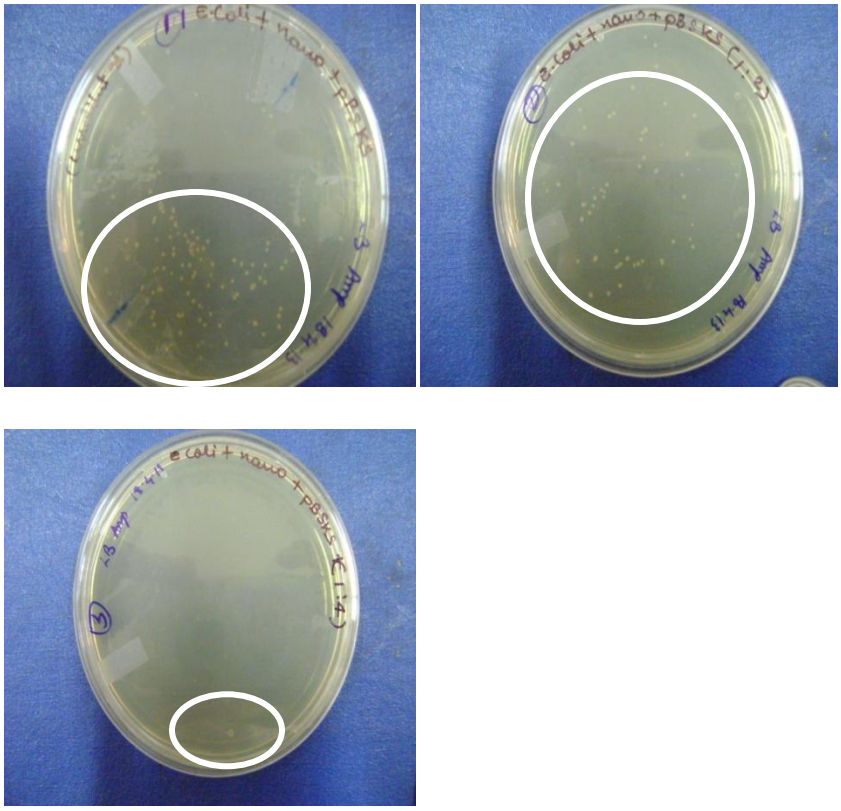

Figure: 6.8 Growth of antibiotic sensitive *E. coli* DH5α in diluted LB broth, containing ampicillin after 1 day incubation with Plasmid loaded nanoparticles.

Conclusion

Iron oxide nanoparticles were successfully synthesized by simple precipitation method. These NPs were employed as gene-delivery vehicles to load pDNA such as pUC18 carrying ampicillin resistance genes. This NPs-conjugated pDNA was

successfully and integrally transfected into E. coli DH5α bacterial cells. From this study it can be concluded that: (i) pDNA makes stable bonding with nanoparticles on its surface by intermolecular H-bonding or simply entrapped inside cavities; (ii) the greater the size of the plasmid, the faster is its release profile. Hence iron oxide nanoparticles can serve as non-toxic, biodegradable and safe vector to load variety of genes of useful products like enzymes, proteins, peptides, hormones etc into bacterial cells. Such a carrier can also be used for delivering genes into eukaryotic cells and can be a potential candidate for use in gene therapy. This work may further be extended in the fields such as bio-augmentation, DNA profiling, development of biosensors.

References:

1. *Compacted DNA nanoparticles administered to the nasal mucosa of cystic fibrosis subjects are safe and demonstrate partial to complete cystic fibrosis transmembrane regulator reconstitution.* Konstan MW, Davis PB, Wagener JS, Hilliard KA, Stern RC, Milgram LJ, Kowalczyk TH, Hyatt SL, Fink TL, Gedeon CR, Oette SM, Payne JM, Muhammad O, Ziady AG, Moen RC, Cooper MJ. 2004, Hum Gene Ther., Vol. 15, pp. 1255-1269.

2. *The development of human gene therapy.* editor., Friedmann T. NY : Cold Spring Harbor Laboratories Press., 1999, p. 729.

3. *Barriers to Nonviral Gene Delivery.* C M WIETHOFF, C R MIDDAUGH. 2003 , JOURNAL OF PHARMACEUTICAL SCIENCES, Vol. 92, pp. 203-217.

4. *substrate specificity and kinetics of degradation of antisense oligonucleotide by a 3 exonuclease.* Eder PS, Rene JD, Dagle JM, Waldereder JA. 1, 2009, Antisense Res Dev, pp. 141–151.

5. *Artificial viruses:a nanotechnological approach to gene delivery.* Mastrobattista E, Van Der AM, Hennink W, Crommelin DJ. 2006, Nat Rev Drug Discov, Vol. 5, pp. 115-121.

6. *Adverse effects of gene therapy: Gene therapy can cause leukaemia: no shock, mild horror but a probe.* ME., Gore. 2003, Gene Ther, Vol. 10, p. 4.
7. *Expression of DNA transferred into mammalian cells.* Rauth S, Kucherlapati RS. 1984, J Biosci, Vol. 6, pp. 543-567.

8. *Human gene therapy.* WF., Anderson. 1998, Nature, Vol. 392, pp. 25–30.

9. *State-of-the-art gene-based therapies: the road ahead.* . Kay, M. A. (2011), Nature Rev. Genet., Vol. 12, pp. 316–328.

10. *Therapeutic in vivo gene transfer for genetic disease using AAV: progress and challenges.* . Mingozzi, F. & High, K. A. (2011), Nature Rev. Genet., Vol. 12, pp. 341–355.

11. *Challenges and strategies: The imimmuneresponses in gene therapy.* Zhou H–S, Liu D–P, Liang C–C. 2004, Med Res Rev, Vol. 24, pp. 748–761.

12. *Report of a second serious adverse event in a clinical trial of gene therapy for X-linked severe combined immune deficiency (X-SCID). Position of the European Society of Gene Therapy (ESGT).* . B., Gansbacher. 2003, J Gene Med, Vol. 5, pp. 261–262.

13. *Knocking down barriers: advances in siRNA delivery.* Whitehead, K. A., Langer, R. & Anderson, D. G. (2009), Nature Rev. Drug Discov. , Vols. 8, , pp. 129–138.

14. *Cationic liposomal lipids: from gene carriers to cell Cationic liposomal lipids: from gene carriers to cell signaling.* . Lonez, C., Vandenbranden, M. & Ruysschaert, J. M. (2008), Prog. Lipid Res. , Vol. 47, pp. 340–347.

15. *Model nucleoprotein complexes: studies on the interaction of cationic homopolypeptides with DNA.* Olins, D. E., Olins, A. L. & Von Hippel, P. H. 1967, J. Mol. Biol., Vol. 24, pp. 157-176.

16. *Characterization of DNA condensates induced by poly(ethylene oxide) and polylysine.* Laemmli, U. K. 1975, Proc. Natl Acad. Sci. USA, Vol. 72, pp. 4288-4292.

17. *Characterization of vectors for gene therapy formed byself-assembly of DNA with synthetic block co-polymers.* Wolfert MA, Schacht EH, Toncheva V, Ulbrich K, Nazarova O, Seymour LW. 1996, Hum Gene Ther, Vol. 7, pp. 2123-2133.

18. *Polyethylenimine-based non-viral gene delivery systems.* Lungwitz, U., Breunig, M., Blunk, T., Gopferich, A. 2005, Eur. J. Pharm. Biopharm. , Vol. 60, pp. 247-266.

19. *A versatile vector for gene and oligonucleotide transfer into cells in culture and in vivo: Polyethylenimine.* BOUSSIF, O., LEZOUALC'H, F., ZANTA, M A., MERGNY, M D., SCHERMAN, D., DEMENEIX, B., BEHR. J -P. 1995, Proc. Natl. Acad. Sci. USA, Vol. 92, pp. 7297-7301.

20. *Size matters: molecular weight affects the efficiency of poly(ethylenimine) as a gene delivery vehicle.* Godbey, W. T., Wu, K. K., Mikos, A. G. 1999, J. Biomed. Mater. Res. 45, 268–275 (1999)., Vol. 45, pp. 268-275.

21. *Different behavior of branched and linear polyethylenimine for gene delivery in vitro and in vivo.* Wightman. L., Kircheis. R., Rössler. V., Carotta. S., Ruzicka. R., Kursa. M., Wagner. E. 2001, Vol. 3, pp. 362-372.

22. *Development of a safe gene delivery system using biodegradable polymer, poly[α-(4-aminobutyl)-l-glycolic acid]*. Lim Y–B, Kim C–H, Kim K, Sim SW, Park J–S. 2000, J Am Chem Soc , Vol. 122, pp. 6524-6525.

23. *Design and development of polymers for gene delivery.* Pack, D. W., Hoffman, A. S., Pun, S. & Stayton, P. S. 2005, Nature Rev. Drug Discov. , Vol. 4, pp. 581-593.

24. *Nonviral vectors for gene delivery.* . Mintzer, M. A. & Simanek, E. E. 2009, Chem. Rev., Vol. 109, pp. 259-302.

25. *Structural effect of carbohydrate containing polycations on gene delivery. 3. Cyclodextrin type and functionalization.* . Popielarski SR, Mishra S, Davis ME. 2003, Bioconjugate Chem, Vol. 14, pp. 672–678.

26. *Cyclodextrins in non-viral gene delivery. ;.* W-F., Lai. 2014, Biomaterials, Vol. 35, pp. 401-411.

27. *Chitosans for gene delivery.* Rev, Borchard G. 2001, Adv Drug Delivery, Vol. 52, pp. 145-150.

28. *Chemical modification of chitosan as a gene carrier in vitro and in vivo.* Kim T-H, Jiang HL, Jere D, Park I-K, Cho M–H, Nah JW, Choi Y–J, Akaike T, Cho C-S. 2007, Prog Polym Sci 2007;32:726–56., Vol. 32, pp. 726-756.

29. *Transformation of Lactobacillus plantarum by electroporation with in vitro modified plasmid DNA.* Alegrea, M T., Rodríguezb, M.C., Mesasc, J M. 2004, FEMS Microb. Lett., Vol. 241, pp. 73-77.

30. *Novel plasmid transformation method mediated by chrysotile, sliding friction, and elastic body exposure.* Yoshida, N., Nakajima-Kambe T, Matsuki K, Shigeno T. 2007, Anal Chem Insights., Vol. 2, pp. 9-15.

31. *Kinetics and mechanism of plasmid DNA penetration through nanopores.* E. Arkhangelsky, Y. Sefi, B. Hajaj, G. Rothenberg, V. Gitis. 2011, J Memb Sci., Vol. 371, pp. 45-51.

32. *Studies on transformation of Escherichia coli with plasmids.* D., Hanahan. 1983, J Mol Biol. , Vol. 166, pp. 557-580.

33. *A Look at Transformation Efficiencies in E. coli:An Investigation into the Relative Efficiency of E. coli to Take up Plasmid DNA Treated with the Complex Molecular Trivalent Cations Spermine or Spermidine within the Context of the Hanahan Protocol for Tra.* J. Clark, J. Hudson, R. Mak, C. McPherson, C. Tsin. 2002, Exp. Microbiol. Immunol., Vol. 2, pp. 68-80.

34. *Enhancement of transfection by physical concentration of DNA at the cell surface.* Luo D1, Saltzman WM. 2000, Nat Biotechnol. , Vol. 18, pp. 893-895.

35. *Nanomagnetism and spin electronics: materials, microstructure and novel properties.* K. M. Krishnan, A. B. Pakhomov, Y. Bao, P. Blomqvist, Y. Chun, M. Gonzales, K. Griffin, X. Ji, B. K. Roberts. 2006, , J Mat Sci, Vol. 41, pp. 793–815.

36. *Improved M13 phage cloning vectorsand host strains: nucleotide sequencing of the M13mp18 and pUC9 vectors.* C. Yanisch-Perron, J. Vieira,J. Messing. 1985, Gene , Vol. 33, pp. 103-119.
37. *Influence of the zeta potential on the sorption and toxicity of iron oxide nanoparticles on S. cerevisiae and E. coli.* H. Schwegmann, A. J. Feitz, F. H. Frimmel. 2010, J. colloid Interface Sci., Vol. 347, p. 43.

38. *Transfecting pDNA to E. coli DH5α using bovine serum albumin nanoparticles as a delivery vehicle.* J.
Wagh, K J Patel, P Soni, K Desai, P Upadhyayd, H. P. Soni. 2015, Luminescence , Vol. 30, pp. 583–591.